

## Amplitude preprocessing of single and multicomponent seismic data

C. P. A. Wapenaar\*, D. J. Verschuur\*, and P. Herrmann‡

### ABSTRACT

Whenever the data acquisition is restricted to line surveys rather than areal surveys, seismic processing is necessarily in two dimensions. In this paper it is argued that two-dimensional (2-D) processing is preferably applied *after* transforming the point source responses into line source responses. The effect of this transformation is a correction of the amplitudes in the data. For single-component acoustic data as well as for multicomponent elastic data a line source response is nothing but a superposition of point source responses. Hence, in principle a line source response can be synthesized by integrating point source responses along the desired line source axis. In practice, however, this integration cannot be carried out due to the incompleteness of the data. It is shown that the integration along the source axis can be replaced by an integration along the receiver axis. The underlying assumption is that the wavefields exhibit a certain type of cylindrical symmetry. For horizontally layered acoustic and elastic media this assumption is fully satisfied. For 2-D inhomogeneous media this assumption is approximately satisfied, provided the data are sorted in CMP gathers. Having transformed the point source responses into line source responses, the results may be considered as "true amplitude" 2-D data. Hence, proceeding with existing 2-D seismic processing techniques is then justified.

### INTRODUCTION

By nature, amplitudes in seismic data depend largely on the three-dimensional (3-D) expansion of seismic waves during propagation (Newman, 1973). As a consequence, 3-D seismic processing is required if we want to fully exploit the

amplitude information contained in the seismic data. Even though in the eighties there has been an important shift toward 3-D seismic data acquisition and processing, a significant part of seismic data acquisition and processing is still two-dimensional (2-D). This applies particularly to the multicomponent situation. The shortcomings of 2-D seismic processing with respect to structural imaging (migration) are well known and are not discussed here.

This paper deals with the shortcomings of 2-D seismic processing with respect to amplitude handling. The underlying assumption of any 2-D seismic processing technique is that the subsurface parameters as well as the seismic wavefield are 2-D functions of the horizontal coordinate ( $x$ ) and the depth coordinate ( $z$ ). This implies that the seismic waves are assumed to be generated by *line sources* (along the  $y$ -axis) rather than *point sources*. Hence, in 2-D processing the amplitudes in the seismic data are treated as if they depend on 2-D rather than 3-D expansion of seismic waves. Needless to say, this yields erroneous amplitudes in the processed seismic data.

In this paper, we develop an *amplitude preprocessing* procedure which transforms point source responses into line source responses. By applying this procedure, the amplitude handling of any 2-D seismic processing technique may be validated. This is not only true for inversion techniques like prestack migration, but also for advanced preprocessing techniques like elastic wavefield decomposition and multiple elimination, as well as for postprocessing techniques like stratigraphic elastic and lithologic inversion.

### FROM POINT SOURCES TO LINE SOURCES

The principle of transforming a point source response into a line source response is simple: as a line source may be seen as a distribution of point sources along a line (Figure 1a), a line source response is nothing but a superposition of point source responses. The only assumption is that the point source responses are described by a linear wave equation

Presented at the 60th Annual International Meeting, Society of Exploration Geophysicists. Manuscript received by the Editor February 7, 1991; revised manuscript received December 18, 1991.

\*Laboratory of Seismics and Acoustics, Delft University of Technology, P.O. Box 5046, 2600 GA Delft, The Netherlands.

‡Formerly Laboratory of Seismics and Acoustics, Delft University of Technology, Delft, The Netherlands; presently Compagnie Générale de Géophysique, 1, Rue Léon Migaux, 91341 Massey Cedex, France.

© 1992 Society of Exploration Geophysicists. All rights reserved.

(acoustic or elastic). For a continuous distribution of point sources along the  $y$ -axis, the superposition principle may be mathematically formulated as

$$\hat{p}(x_r, z_r; x_s, z_s; t) = \int_{-\infty}^{\infty} p(x_r, y_r = 0, z_r; x_s, y_s, z_s; t) dy_s, \quad (1)$$

where  $p(x_r, y_r, z_r; x_s, y_s, z_s; t)$  is a point source response as a function of time ( $t$ ) at receiver point  $(x_r, y_r, z_r)$  for a point source at  $(x_s, y_s, z_s)$  and where  $\hat{p}(x_r, z_r; x_s, z_s; t)$  is a line source response at receiver point  $(x_r, y_r = 0, z_r)$  for a line source at  $(x_s, z_s)$ . When the medium parameters are independent of the  $y$ -coordinate, the response of a point source at  $(x_s, y_s, z_s)$  is just a shifted version of the response of a point source at  $(x_s, 0, z_s)$ :

$$p(x_r, y_r, z_r; x_s, y_s, z_s; t) = p(x_r, y_r - y_s, z_r; x_s, 0, z_s; t). \quad (2)$$

Substitution in equation (1) yields

$$\hat{p}(x_r, z_r; x_s, z_s; t) = \int_{-\infty}^{\infty} p(x_r, -y_s, z_r; x_s, 0, z_s; t) dy_s, \quad (3a)$$

or, renaming the integration variable,

$$\hat{p}(x_r, z_r; x_s, z_s; t) = \int_{-\infty}^{\infty} p(x_r, y_r, z_r; x_s, 0, z_s; t) dy_r. \quad (3b)$$

The latter equation states that the line source response  $\hat{p}(x_r, z_r; x_s, z_s; t)$  may be synthesized from a *single* point source response by carrying out an integration along the receiver coordinate  $y_r$ . The principle is visualized in Figure 1b. Bear in mind that equation (3b) holds for any 2-D inhomogeneous acoustic or elastic medium. However, equation (3b) is not yet suited for practical situations where the response is measured for  $y_r = 0$  only. When the response satisfies certain symmetry properties in the  $x_r, y_r$ -plane, the integral

(3b) along the receiver coordinate  $y_r$  may be replaced by an integral along the receiver coordinate  $x_r$ . The simplest situation occurs in the case of an acoustic response of a horizontally layered medium. This situation is studied in the next section. More complicated forms of symmetry occurring for multicomponent elastic data are studied in the subsequent sections.

HORIZONTALLY LAYERED ACOUSTIC MEDIUM

Consider a horizontally layered acoustic medium bounded by a free surface at  $z = z_0$  with a point source at  $(x = 0, y = 0, z = z_s)$ . Let  $p(x, y, z_r, t)$  denote the acoustic response at receiver depth level  $z_r$  as a function of  $x, y$  and  $t$  (for notational convenience the source point coordinates are omitted). With this simplified notation, equation (3b) reads

$$\hat{p}(x, z_r, t) = \int_{-\infty}^{\infty} p(x, y, z_r, t) dy. \quad (4)$$

Throughout this section,  $p$  may either represent the acoustic pressure below the free surface or the vertical component of the particle velocity at (or below) the free surface. For both situations, the response exhibits cylindrical symmetry with respect to the  $z$ -axis. Hence, at the receiver depth level  $z_r$  at a fixed time  $t$ ,  $p(x, y, z_r, t)$  is constant on circles described by

$$\sqrt{x^2 + y^2} = \text{constant}, \quad (5)$$

see Figure 2a.

Hence, if the response is measured only for  $y = 0$ , the unknown response at  $(x, y, z_r)$  should be expressed in terms of the measured response at  $(\rho, 0, z_r)$ , according to

$$p(x, y, z_r, t) = p(\rho, 0, z_r, t), \quad (6a)$$

where

$$\rho = \sqrt{x^2 + y^2}. \quad (6b)$$

Let  $\rho$  be the new integration variable. Then

$$d\rho = \frac{\sqrt{\rho^2 - x^2}}{\rho} dy. \quad (6c)$$

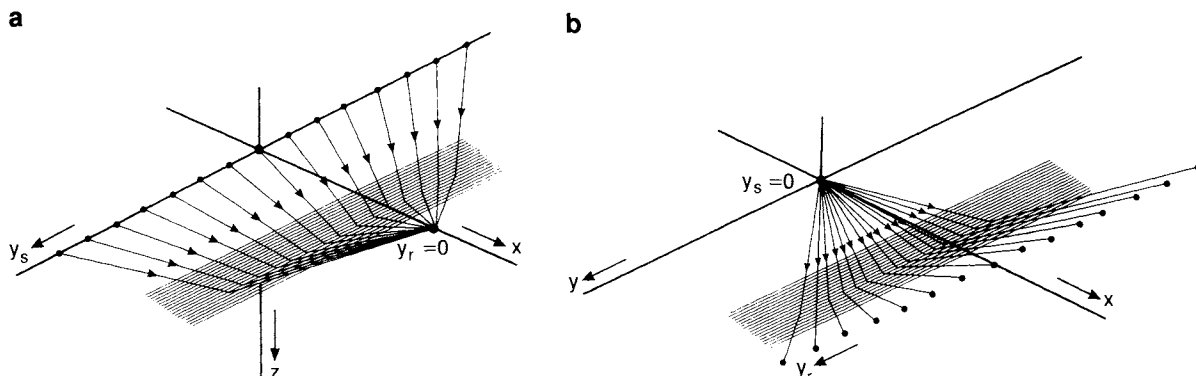


FIG. 1. (a) A line source response is obtained from many point source responses by integration along the source coordinate  $y_s$ . (b) For any 2-D inhomogeneous medium, a line source response may be obtained from one point source response by integration along the receiver coordinate  $y_r$ .

The integration along the  $y$ -axis in equation (4) may thus be replaced by an integration along the  $\rho$ -axis, according to

$$\hat{p}(x, z_r, t) = 2 \int_{|x|}^{\infty} p(\rho, 0, z_r, t) \frac{\rho}{\sqrt{\rho^2 - x^2}} d\rho, \quad (7)$$

see Figure 2b. Equation (7) is the basis for transforming the acoustic point source response  $p(\rho, 0, z_r, t)$  into an acoustic line source response  $\hat{p}(x, z_r, t)$  (amplitude preprocessing). The principle of this *lateral filtering procedure* is visualized in Figure 3.

It is interesting to note that the main contribution to the integral comes from the first Fresnel zone starting at  $\rho = |x|$ , the contributions of the higher Fresnel zones cancel (compare with diffraction theory). A direct consequence is that the assumed cylindrical symmetry is actually required only for a small range of azimuth angles. Moreover, in practical situations the infinite integration interval in equation (7) may be replaced by a finite interval without losing much accuracy, particularly when a taper is used at the upper integration limit. In situations with noise, the integration interval chosen should be as narrow as possible (but containing at least one Fresnel zone). The square root singularity at the lower integration limit needs special attention. Stability is guaranteed when using the numerical integration procedure as discussed in Fokkema et al. (1992).

An interesting aspect of the proposed method is that it can handle both primaries and multiple reflections since both types of reflections fulfill the cylindrical symmetry assumption. Another interesting aspect is that the method can properly handle crossing events, unlike the time-dependent scaling procedure that is generally used in practice. This is illustrated in Figures 4, 5 and 6. Figure 4 shows modeled data (primaries only) for an acoustic two layer model. The two data sets represent a point source and a line source response. The point source response (Figure 4a) is the input for our test, the modeled line source response (Figure 4b) serves as a reference for the output of our test. Figure 5 shows the results of two ways of amplitude preprocessing. Figure 5a was obtained by scaling the data with the square root of the

travel time. Note that at the crossing point both events were scaled with the same factor, which is erroneous for the second event. Figure 5b is the result of our lateral filtering procedure. At the crossing point, the two events were weighted differently due to their different time dips. This can be seen more clearly in Figure 6, which shows amplitude cross sections of the data in Figures 4 and 5. Figure 6a shows that the amplitudes of the first event were properly corrected by both methods, which is not surprising because the medium above the first reflector is homogeneous. For the second event, Figure 6b shows that the lateral filtering procedure is superior to the temporal scaling procedure [remember that equation (7) is exact].

RELATION WITH PLANE-WAVE DECOMPOSITION

For a horizontally layered medium, seismic inversion is often applied after plane-wave decomposition. Decomposition of a *line source* response into monochromatic plane waves is described mathematically by a double Fourier transform (Berkhout, 1985), according to

$$\hat{P}(k_x, z_r, \omega) = \int_{-\infty}^{\infty} e^{-i\omega t} dt \int_{-\infty}^{\infty} \hat{p}(x, z_r, t) e^{ik_x x} dx, \quad (8a)$$

with

$$i = \sqrt{-1}. \quad (8b)$$

For each  $k_x$  and  $\omega$  value,  $\hat{P}(k_x, z_r, \omega)$  represents the complex amplitude of a monochromatic plane wave with angular frequency  $\omega$  and dip angle  $\alpha$ , such that

$$k_x = \frac{\omega}{c(z_r)} \sin \alpha, \quad (9)$$

where  $c(z_r)$  is the propagation velocity at the receiver depth level  $z_r$ . Note that equations (7) and (8) together may be seen as a two-step procedure for decomposing a *point source* response into monochromatic plane waves (Figure 7a).

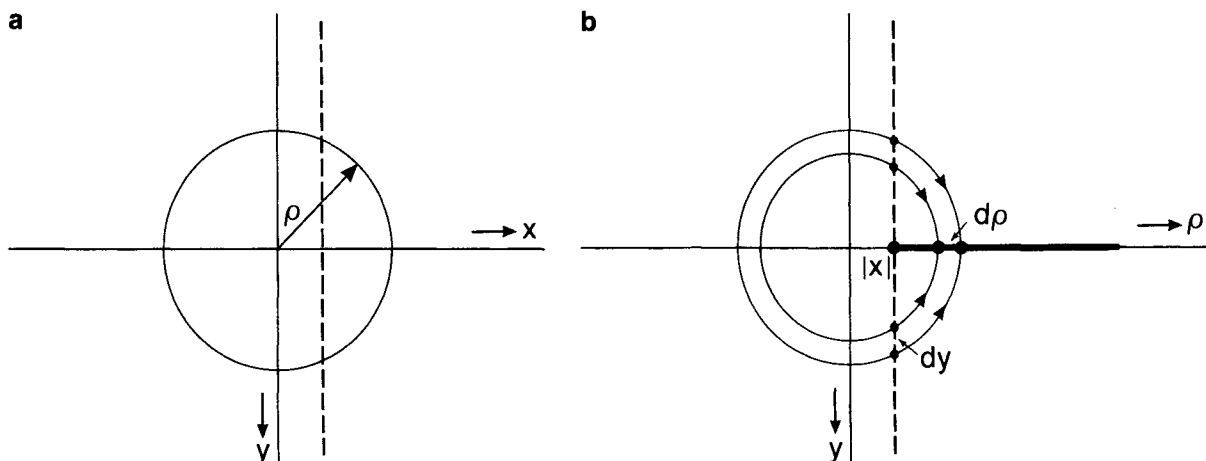


FIG. 2. (a) Plan view of Figure 1b: cylindrical symmetry assumption. (b) Coordinate transformation. Assuming cylindrical symmetry, the integration along the  $y$ -axis for fixed  $x$  (dashed line) may be transformed into an integration along the  $\rho$ -axis, starting at  $|x|$  (solid line). The scaling factor  $\rho/\sqrt{\rho^2 - x^2}$  in equation (7) accounts for the ratio  $dy/d\rho$ .

Downloaded 11/29/23 to 145.90.34.119. Redistribution subject to SEG license or copyright; see Terms of Use at http://library.seg.org/page/policies/terms DOI:10.1190/1.1443331

Hence, equations (7) and (8) together have the same effect as a Fourier-Hankel transform (Treitel et al., 1982),

$$\hat{P}(k_x, z_r, \omega) = 2\pi \int_{-\infty}^{\infty} e^{-i\omega t} dt \int_0^{\infty} p(\rho, 0, z_r, t) J_0(k_x \rho) \rho d\rho, \quad (10)$$

where  $J_0$  is the zeroth order Bessel function (Figure 7b). The proof is given in the Appendix. Brysk and McCowan (1986) first showed that a Hankel transform may be efficiently implemented as a Fourier transform, followed by a square-root filter. Their approach was later improved by Fokkema et al. (1991). From the above analysis, it follows that, alternatively, a Hankel transform may be implemented as a square-root filter, followed by a Fourier transform. From a computational point of view, both approaches are equivalent. However, in the latter approach, the square-root filter described by equation (7) has a clear physical meaning: it transforms a point source response of a horizontally layered acoustic medium into a line source response. In the following sections several variants of equations (7) are studied for different configurations.

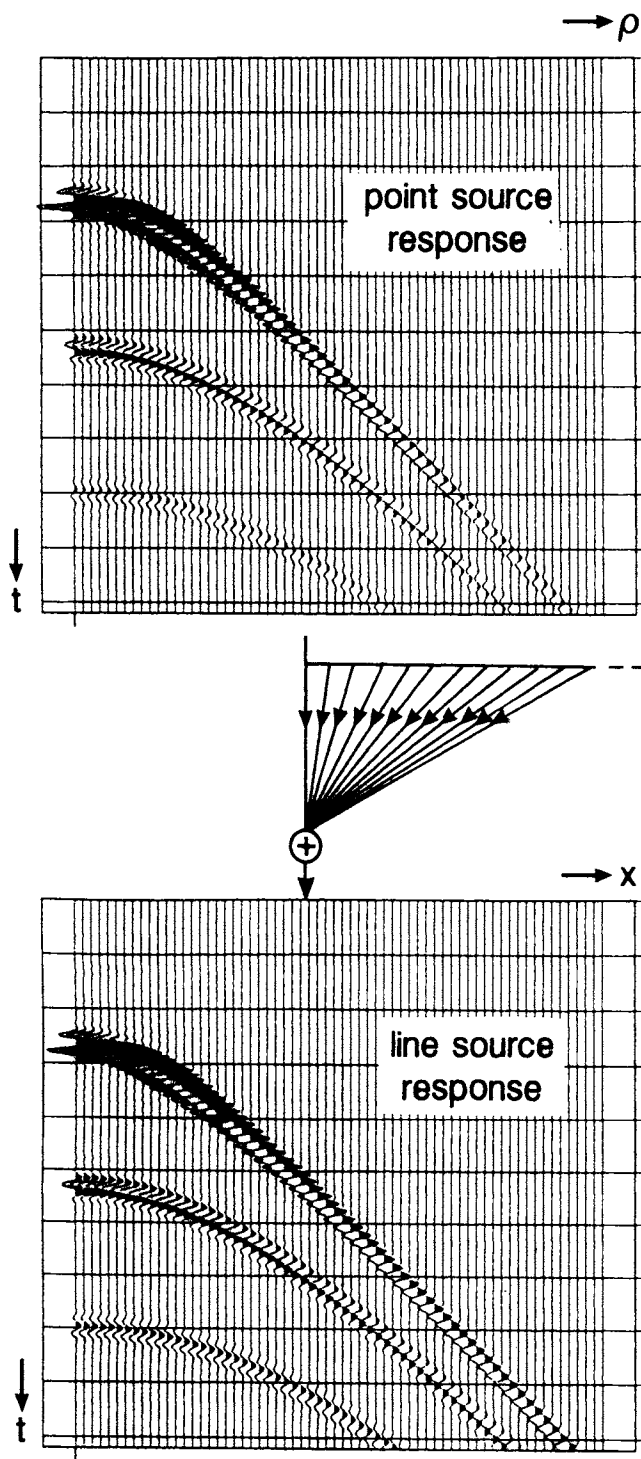


FIG. 3. According to equation (7), one trace of an acoustic line source response is obtained as a weighted addition of traces of an acoustic point source response (lateral filtering).

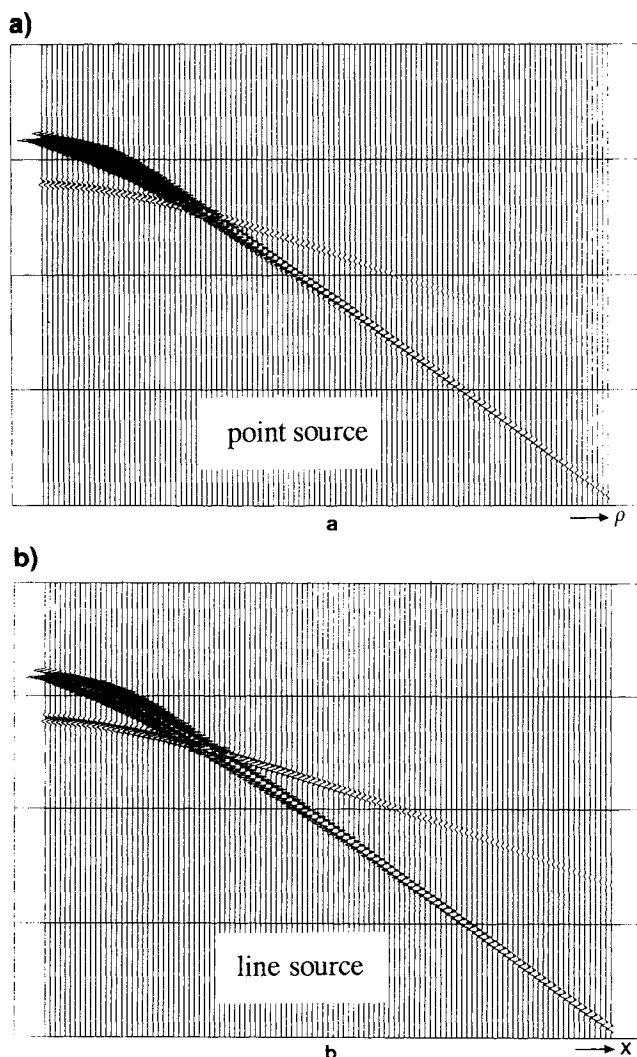


FIG. 4. Modeled data (primaries only) for an acoustic two-layer model (velocities 1500 m/s and 3000 m/s; mass densities 1000 kg/m<sup>3</sup> and 2000 kg/m<sup>3</sup>; layer thicknesses 300 m each).

## 2-D INHOMOGENEOUS ACOUSTIC MEDIUM

The underlying assumption of equation (7) is that the acoustic response is cylindrically symmetric with respect to the  $z$ -axis. For an arbitrary 2-D inhomogeneous acoustic medium this assumption is violated.

A partial remedy is given by the following procedure:

- 1) Resort the common source point (CSP) gathers into common midpoint (CMP) gathers. Note that CMP gathers are symmetric in  $\rho$ , where  $\rho$  now stands for source-receiver offset.
- 2) Consider each CMP gather as a point source response of a horizontally layered medium and simulate line source responses by applying equation (7) to each CMP gather.
- 3) Resort the CMP gathers into CSP gathers.

To understand the principle of this procedure, let us first consider a situation with a single dipping interface (dip angle  $\alpha$ ), underlying a homogeneous layer (velocity  $c$ ). The configuration for a CMP gather (i.e., the result of step 1) is

shown in Figure 8a. The traveltime  $T(h)$  as a function of the half offset  $h$  is given by (Levin, 1971):

$$T^2(h) = T^2(0) + \frac{4h^2 \cos^2 \alpha}{c^2}. \quad (11)$$

Figure 8b shows the configuration for an equivalent CSP gather over a horizontal interface underlying a homogeneous layer (velocity  $c/\cos \alpha$ ). This CSP gather is equivalent to the CMP gather in the sense that the traveltimes are again described by equation (11). Furthermore, the incidence angle  $\beta$  at the interface is identical in both situations, meaning that the amplitude versus offset (AVO) effects are also the same. Table 1 gives an overview of the analytic amplitudes, both for a point source and a line source response (far field approximation). In step 2 of the proposed procedure the configuration of Figure 8b is assumed, hence the data are effectively scaled by a factor  $(c/\cos \alpha)(2\pi T(h)/i\omega)^{1/2}$ , see Table 1. However, the actual configuration is given by Figure 8a and the desired effective scaling factor is  $c(2\pi T(h)/i\omega)^{1/2}$ , again see Table 1.

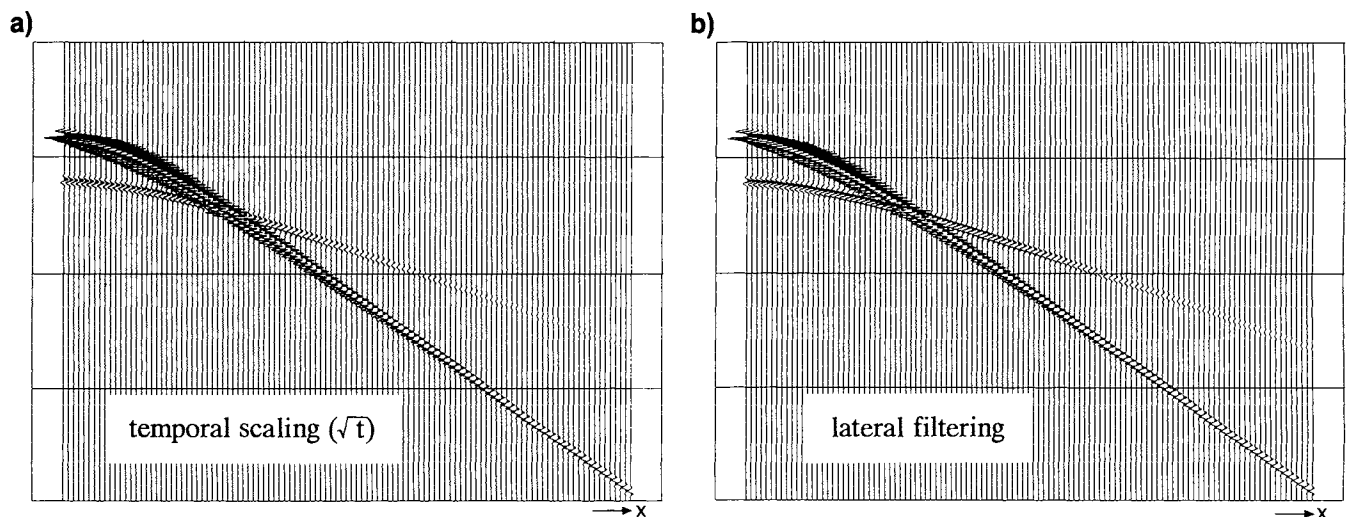


FIG. 5. Amplitude preprocessing applied to the point source response of Figure 4a. These results should be compared with the modeled line source response of Figure 4b.

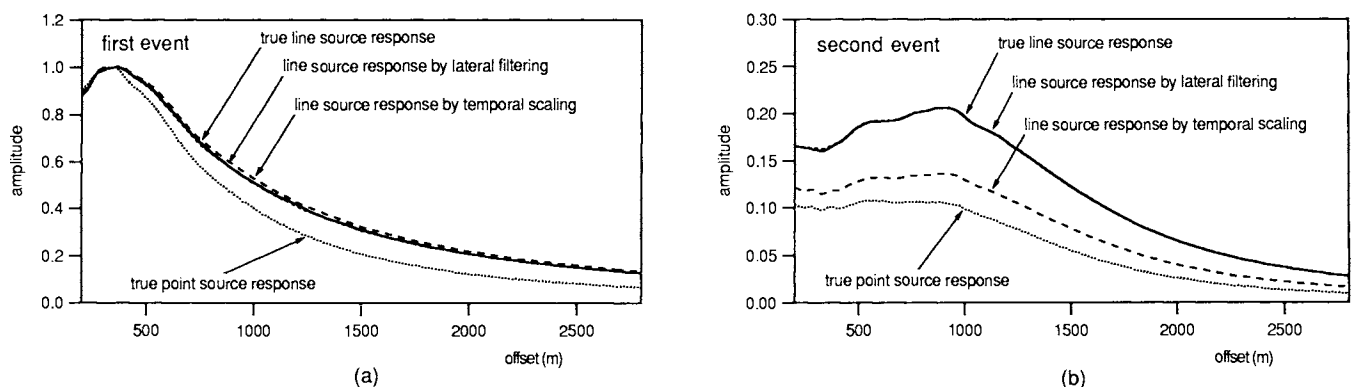


FIG. 6. Model with two reflectors. Amplitude cross sections of the data in Figures 4 and 5.

Hence, applying the proposed procedure yields a line source response with amplitudes that are a factor  $1/\cos \alpha$  too high. Fortunately this factor is independent of the half offset  $h$ . Consequently, for this simple configuration, the transformed data will contain the correct AVO effects, irrespective of the magnitude of the dip angle  $\alpha$ .

Next consider a layered medium with dipping interfaces, as shown in Figure 9a. We modeled the CMP response of the third reflector by ray tracing. The "true" amplitudes for the situation with point sources as well as line sources were computed with the method of stationary phase, see Figure 9b. The amplitudes of the line source response, obtained by applying our lateral filtering procedure to the point source response, are also shown in Figure 9b. Note that this result, which was scaled for display purposes by a constant factor

0.95, matches well with the amplitudes of the true line source response.

Finally, note that the accuracy of our lateral filtering procedure decreases for increasing complexity of the medium; for very complex media, 3-D acquisition and processing is the only acceptable approach.

HORIZONTALLY LAYERED ELASTIC MEDIUM

Consider a horizontally layered isotropic elastic medium bounded by a free surface at  $z = z_0$  with a point force at  $(x = 0, y = 0, z = z_s)$ . Let  $v_{i,j}(x, y, z_r, t)$  denote the multicomponent response at receiver depth level  $z_r$ , as a function of  $x, y$ , and  $t$ . The subscripts  $i$  and  $j$  may stand for

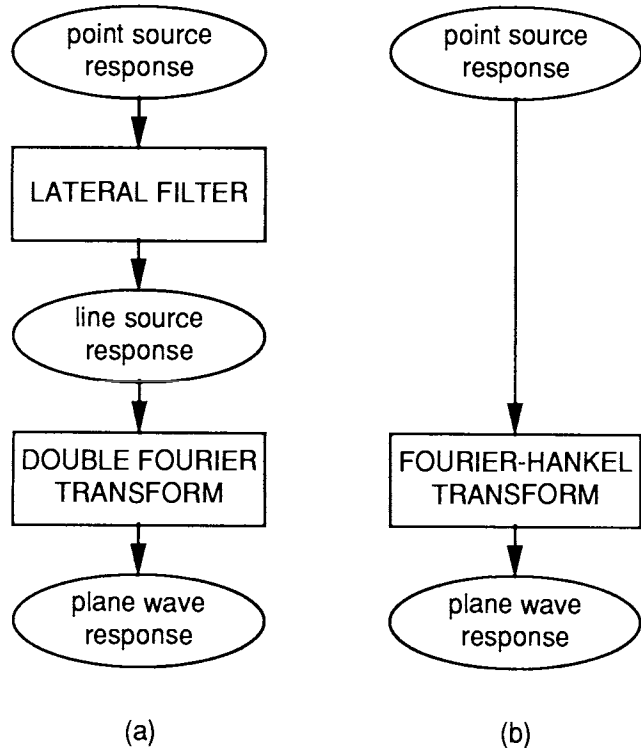


FIG. 7. (a) Lateral filtering as one step in a plane-wave decomposition process. (b) Plane-wave decomposition by Fourier-Hankel transformation.

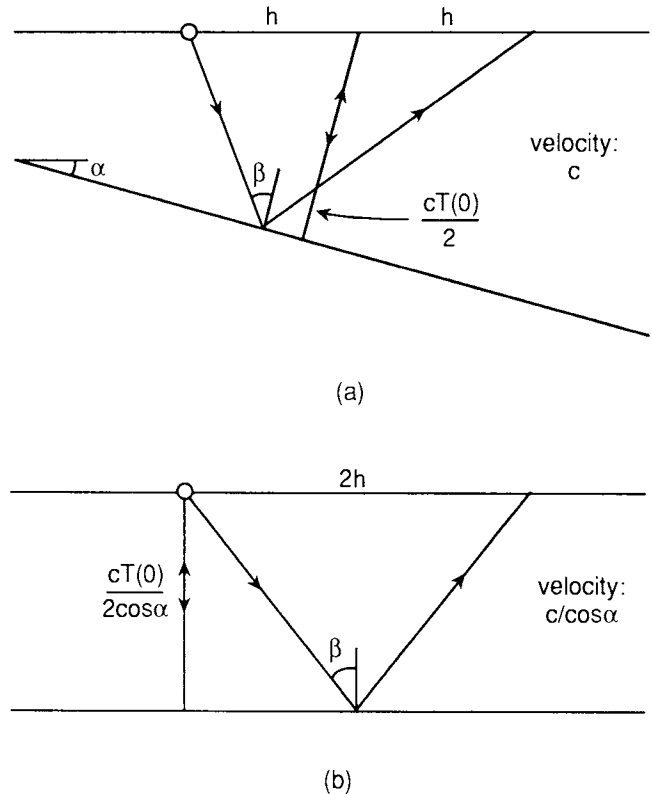


FIG. 8. When the cylindrical symmetry is not fulfilled the amplitude transformation should be applied to CMP gathers. (a) CMP configuration for a single dipping interface. (b) Equivalent CSP configuration for a horizontal interface.

Table 1. Analytic amplitudes for the CMP configuration of Figure 8a and the equivalent CSP configuration of Figure 8b (far-field approximation).

	Point source response	Line source response	Effective scaling factor
CMP, velocity $c$ (Figure 8a)	$\frac{R(\beta)^*}{4\pi c T(h)}$	$\frac{R(\beta)}{\sqrt{8\pi i \omega T(h)}}$	$c \sqrt{\frac{2\pi T(h)}{i \omega}}$
CSP, velocity $c/\cos \alpha$ (Figure 8b)	$\frac{\cos \alpha R(\beta)}{4\pi c T(h)}$	$\frac{R(\beta)}{\sqrt{8\pi i \omega T(h)}}$	$\frac{c}{\cos \alpha} \sqrt{\frac{2\pi T(h)}{i \omega}}$

\*Angle dependent reflection coefficient.

$x$ ,  $y$ , or  $z$ . The first subscript  $i$  refers to the direction of the measured particle velocity at  $(x, y, z_r)$ ; the second subscript  $j$  refers to the direction of the force applied at  $(0, 0, z_s)$ . Using this notation, equation (3b) becomes

$$\hat{v}_{i,j}(x, z_r, t) = \int_{-\infty}^{\infty} v_{i,j}(x, y, z_r, t) dy. \quad (12)$$

If the response  $v_{i,j}(x, y, z_r, t)$  is measured only for  $y = 0$ , the unknown response at  $(x, y, z_r)$  should be expressed in terms of the measured response at  $(\rho, 0, z_r)$ , with  $\rho$  defined in equation (6b). For a homogeneous as well as for a horizontally layered isotropic elastic medium, the symmetry properties of multicomponent seismic data read

$$v_{x,x}(x, y, z_r, t) = v_{x,x}(\rho, 0, z_r, t) \frac{x^2}{\rho^2} + v_{y,y}(\rho, 0, z_r, t) \frac{y^2}{\rho^2}, \quad (13a)$$

$$v_{y,x}(x, y, z_r, t) = [v_{x,x}(\rho, 0, z_r, t) - v_{y,y}(\rho, 0, z_r, t)] \frac{xy}{\rho^2}, \quad (13b)$$

$$v_{z,x}(x, y, z_r, t) = v_{z,x}(\rho, 0, z_r, t) \frac{x}{\rho}, \quad (13c)$$

$$v_{x,y}(x, y, z_r, t) = [v_{x,x}(\rho, 0, z_r, t)$$

$$- v_{y,y}(\rho, 0, z_r, t)] \frac{xy}{\rho^2}, \quad (14a)$$

$$v_{y,y}(x, y, z_r, t) = v_{x,x}(\rho, 0, z_r, t) \frac{y^2}{\rho^2} + v_{y,y}(\rho, 0, z_r, t) \frac{x^2}{\rho^2}, \quad (14b)$$

$$v_{z,y}(x, y, z_r, t) = v_{z,x}(\rho, 0, z_r, t) \frac{y}{\rho}, \quad (14c)$$

$$v_{x,z}(x, y, z_r, t) = v_{x,z}(\rho, 0, z_r, t) \frac{x}{\rho}, \quad (15a)$$

$$v_{y,z}(x, y, z_r, t) = v_{x,z}(\rho, 0, z_r, t) \frac{y}{\rho}, \quad (15b)$$

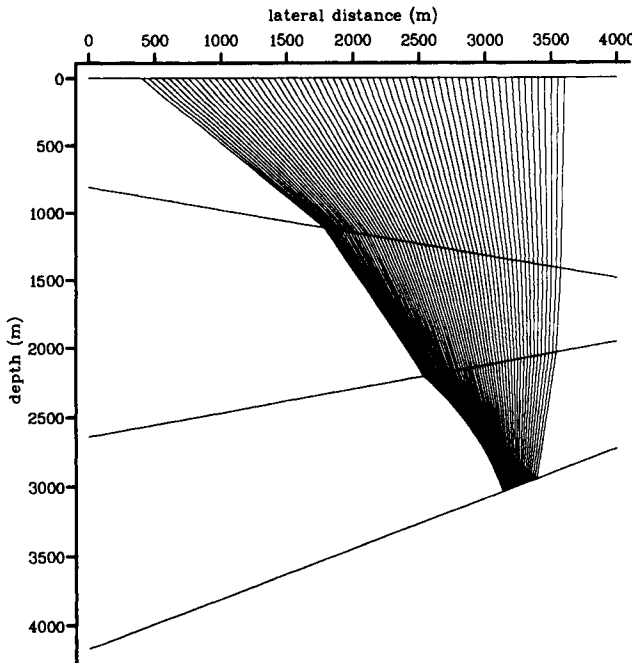
and

$$v_{z,z}(x, y, z_r, t) = v_{z,z}(\rho, 0, z_r, t). \quad (15c)$$

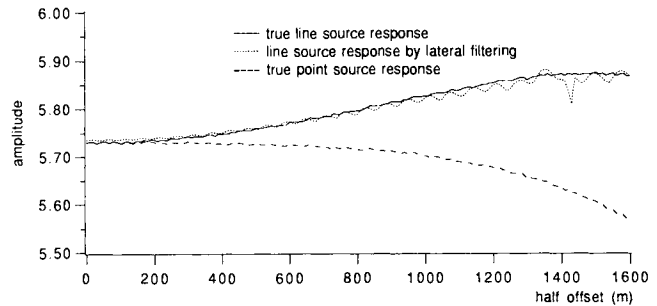
Note that equation (15c) is identical to equation (6a), with  $p$  replaced by  $v_{z,z}$ . Also note that  $v_{x,y}$ ,  $v_{z,y}$ ,  $v_{y,x}$  and  $v_{y,z}$  are odd functions of  $y$ . Hence, substitution into equation (12) yields

$$\hat{v}_{x,y}(x, z_r, t) = \hat{v}_{z,y}(x, z_r, t) = 0 \quad (16a)$$

and



a



b

FIG. 9. Example of amplitude preprocessing for a 2-D inhomogeneous acoustic medium. (a) CMP configuration for a layered medium with dipping interfaces.  $c_1 = 4000$  m/s,  $c_2 = 3200$  m/s,  $c_3 = 4800$  m/s,  $c_4 = 2000$  m/s. (b) Amplitude cross sections for the third reflector. All curves are scaled to the same amplitude at zero offset.

$$\hat{v}_{y,x}(x, z_r, t) = \hat{v}_{y,z}(x, z_r, t) = 0. \quad (16b)$$

Equation (16a) states that the particle velocity in the  $x$ ,  $z$ -plane due to a force in the  $y$ -direction uniformly distributed along the  $y$ -axis equals zero; equation (16b) describes the reciprocal situation. The nonzero line source responses are obtained in a similar way as in the acoustic situation. Substituting equations (13), (14), or (15) into equation (12) and choosing  $\rho$  as the new integration variable, yields in analogy with equation (7)

$$\begin{aligned} \hat{v}_{x,x}(x, z_r, t) = & 2 \int_{|x|}^{\infty} v_{x,x}(\rho, 0, z_r, t) \frac{x^2}{\rho \sqrt{\rho^2 - x^2}} d\rho \\ & + 2 \int_{|x|}^{\infty} v_{y,y}(\rho, 0, z_r, t) \frac{\sqrt{\rho^2 - x^2}}{\rho} d\rho, \quad (17a) \end{aligned}$$

$$\begin{aligned} \hat{v}_{y,y}(x, z_r, t) = & 2 \int_{|x|}^{\infty} v_{x,x}(\rho, 0, z_r, t) \frac{\sqrt{\rho^2 - x^2}}{\rho} d\rho \\ & + 2 \int_{|x|}^{\infty} v_{y,y}(\rho, 0, z_r, t) \frac{x^2}{\rho \sqrt{\rho^2 - x^2}} d\rho, \quad (17b) \end{aligned}$$

$$\hat{v}_{z,z}(x, z_r, t) = 2 \int_{|x|}^{\infty} v_{z,z}(\rho, 0, z_r, t) \frac{\rho}{\sqrt{\rho^2 - x^2}} d\rho, \quad (17c)$$

$$\hat{v}_{z,x}(x, z_r, t) = 2 \int_{|x|}^{\infty} v_{z,x}(\rho, 0, z_r, t) \frac{x}{\sqrt{\rho^2 - x^2}} d\rho, \quad (17d)$$

and, using reciprocity,

$$\hat{v}_{x,z}(x, z_r, t) = \hat{v}_{z,x}(-x, z_r, t) = -\hat{v}_{z,x}(x, z_r, t). \quad (17e)$$

Equations (17a) to (17e) are the basis for transforming the elastic point source responses  $v_{i,j}(\rho, 0, z_r, t)$  into elastic line source responses  $\hat{v}_{i,j}(x, z_r, t)$ . Note that the point source response  $v_{y,y}$  contributes to the line source response  $\hat{v}_{x,x}$  (equation 17a), and the point source response  $v_{x,x}$  contributes to the line source response  $\hat{v}_{y,y}$  (equation 17b). In Figure 10, it can be seen that these cross terms contribute to the small offsets only.

Note that equation (17c) for transforming the  $v_{z,z}$  data (vertical vibrators, vertical geophones) contains the same weighting function as equation (7) for the acoustic situation. Despite this similarity, the effect of this transformation for elastic  $v_{z,z}$  data is much more important than for acoustic data. This is illustrated in Figures 11 and 12. Figure 11 shows modeled data (primaries only) for an elastic single layer model. The point source response (Figure 11a) is the input for our test, and the modeled line source response (Figure 11b) serves as a reference for the output of our test. Figure 12a was obtained by scaling the data with the square root of the traveltime. Figure 12b is the result of our lateral filtering procedure. Comparing both results with Figure 11b shows

that for this situation the lateral filtering procedure is far superior.

Apparently the conflicting time dips of the  $P$  and  $S$  events are properly handled by the lateral filtering procedure, whereas they are completely ignored by the temporal scaling technique.

## 2-D INHOMOGENEOUS ELASTIC MEDIUM

For a 2-D inhomogeneous elastic medium, equations (17a) to (17e) should be applied after resorting the CSP gathers into CMP gathers. For similar reasons as previously discussed, accurate results may be expected for layered media with gentle lateral inhomogeneities.

## DISCUSSION

Another way of dealing with 3-D amplitudes in 2-D processing was proposed in Bleistein et al. (1987) for the acoustic situation and refined by Geoltrain (1989) for the full elastic situation. They introduced a technique that was called two and one-half dimensional (2.5-D) Born inversion. The underlying assumption of 2.5-D inversion is that the subsurface is 2-D inhomogeneous, whereas the wavefields expand in a 3-D sense. Unlike our amplitude transformation procedure, their method does not rely on (approximate) cylindrical symmetry and is therefore more accurate in the case of significant lateral inhomogeneities. On the other hand, unlike our method, 2.5-D inversion does not cope with surface related phenomena like multiple reflections and conversion. Hence, an important advantage of our amplitude transformation procedure is that it validates the amplitude handling of *any* 2-D processing technique, including advanced preprocessing techniques like elastic wavefield decomposition and wave equation-based multiple elimination, as long as the lateral inhomogeneities are moderate. Remember that in the limiting case of a horizontally layered acoustic or elastic medium our equations (7) and (17) are exact.

## CONCLUSIONS

Amplitude information plays an increasingly important role at all stages of advanced seismic processing and interpretation. Wave equation-based multiple elimination only works properly when the amplitudes of the predicted multiples match the amplitudes of the true multiples (Verschuur et al. 1992). Inverse wavefield extrapolation compensates for, amongst others, geometrical spreading effects, provided the proper operators are used. And, last but not least, true amplitude angle-dependent reflectivity is a prerequisite for determining the detailed  $P$ - and  $S$ -velocities and density in a potential reservoir. The amplitude preprocessing method proposed in this paper validates the 2-D amplitude handling peculiar to any 2-D processing technique. The method essentially comes to a lateral filtering procedure, designed as an accurate alternative to the conventionally used temporal scaling by the square root of the traveltime.

The lateral filtering procedure is exact for acoustic and elastic data over any horizontally layered medium whereas the temporal scaling procedure is exact only for acoustic data over a constant velocity medium. Therefore, particu-

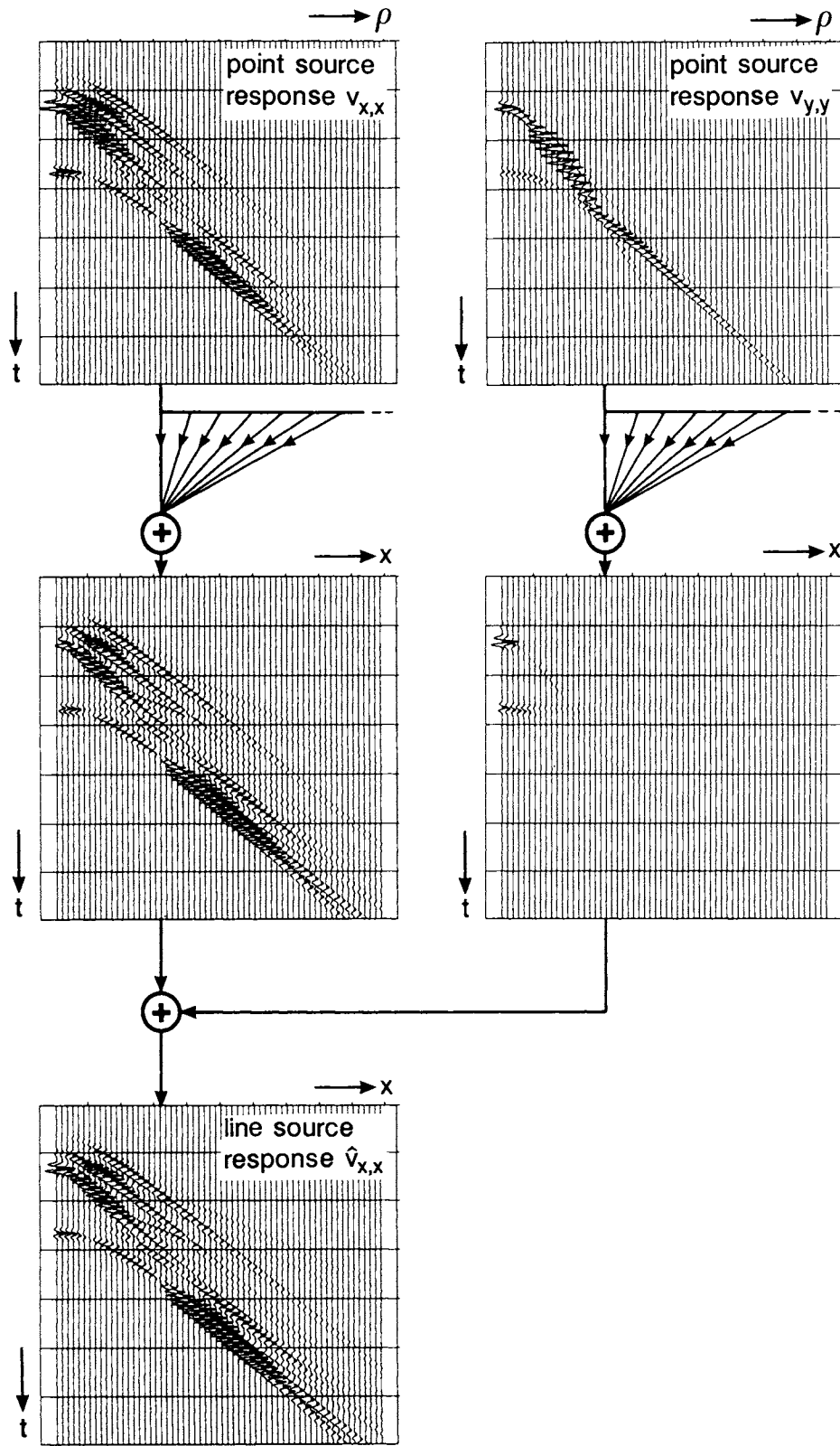


FIG. 10. According to equation (17), one trace of an elastic line source response is obtained as a weighted addition of traces of a multicomponent elastic point source response.

Downloaded 11/29/23 to 145.90.34.119. Redistribution subject to SEG license or copyright; see Terms of Use at http://library.seg.org/page/policies/terms DOI:10.1190/1.1443331

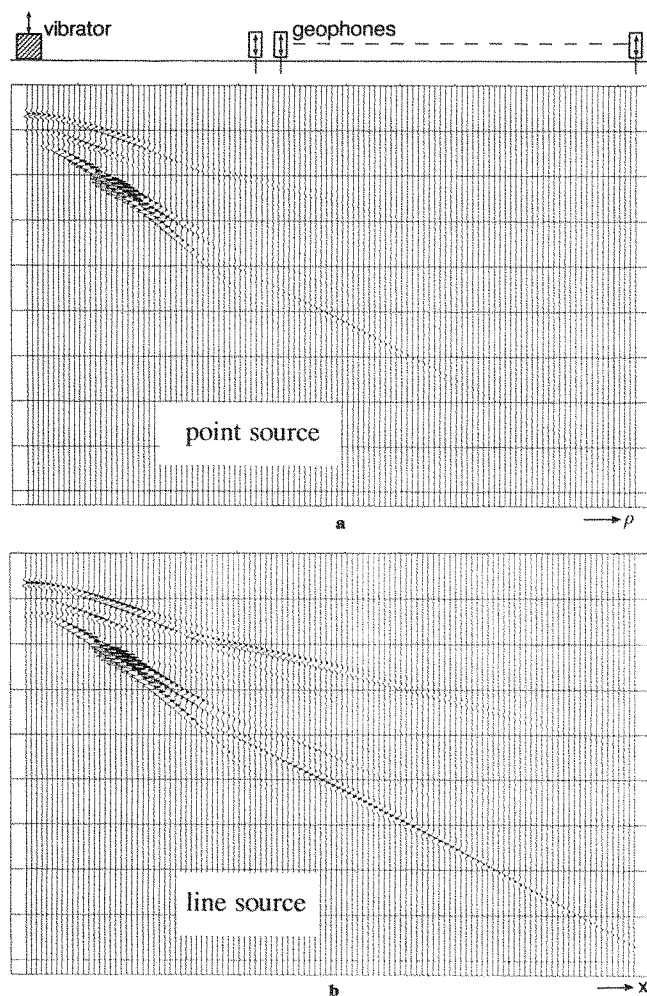


FIG. 11. Modeled data (primaries only) for an elastic two-layer model ( $P$ -velocities 3000 m/s and 5000 m/s;  $S$ -velocities 1500 m/s and 2500 m/s; mass densities 1000 kg/m<sup>3</sup> each; layer thicknesses 600 m and 1000 m).

larly for multicomponent elastic data, the lateral filtering procedure is superior to the temporal scaling method. When applied to CMP gathers, the lateral filtering technique allows gentle lateral inhomogeneities. The accuracy decreases when the complexity of the subsurface increases; for a complex geology the only acceptable solution is given by 3-D acquisition and processing.

#### ACKNOWLEDGMENTS

These investigations were supported by the Royal Dutch Academy of Sciences (C. P. A. Wapenaar), the Dutch Science Foundation (D. J. Verschuur), the Compagnie Générale de Géophysique (P. Herrmann) and the sponsors of the Delphi consortium. We appreciate the assistance of Mrs. D. de Jonge and Mr. M. Teenstra for generating the examples. Stimulating discussions with Dr. J. T. Fokkema are highly appreciated.

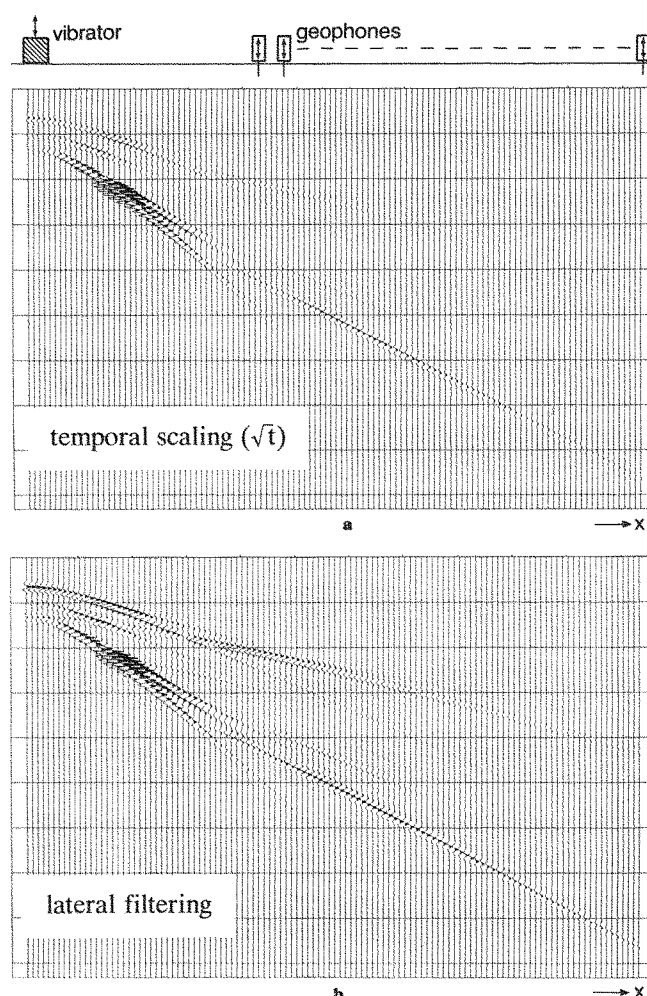


FIG. 12. Amplitude preprocessing applied to the point source response of Figure 11a. These results should be compared with the modeled line source response of Figure 11b.

#### REFERENCES

- Abramowitz, M., and Stegun, I. A., 1970. Handbook of mathematical functions: Dover Publ., Inc.
- Berkhout, A. J., 1985. Seismic migration. Imaging of acoustic energy by wave field extrapolation. A. Theoretical aspects: Elsevier Science Publ. Co., Inc.
- Bleistein, N., Cohen, J. K., and Hagin, F. G., 1987. 2.5-D Born inversion with an arbitrary reference: *Geophysics*, **52**, 26–36.
- Brysk, H., and McCowan, D. W., 1986. A slant-stack procedure for point-source data: *Geophysics*, **51**, 1370–1386.
- Fokkema, J. T., van den Berg, P. M., and Vissinga, M., 1992. On the computation of Radon transforms of seismic data: *J. Seis. Expl.*, **1**, 93–105.
- Geoltrain, S., 1989. Asymptotic solutions to direct and inverse scattering in anisotropic elastic media: Ph.D. thesis, Colorado School of Mines.
- Levin, F. K., 1971. Apparent velocity from dipping interface reflections (common depth-point stacking multiples): *Geophysics*, **36**, 510–516.
- Newman, P., 1973. Divergence effects in a layered earth: *Geophysics*, **38**, 481–488.
- Treitel, S., Gutowski, P. R., and Wagner, D. E., 1982. Plane-wave decomposition of seismograms: *Geophysics*, **47**, 1375–1401.
- Verschuur, D. J., Berkhout, A. J., and Wapenaar, C. P. A., 1992. Adaptive surface-related multiple elimination: *Geophysics*, **57**, 1166–1177.

## APPENDIX

## TWO-STEP HANKEL TRANSFORM

Omitting the temporal Fourier transform for convenience and simplifying the notation, equations (7) and (8) can be combined to

$$\hat{p}(k_x) = 2 \int_{-\infty}^{\infty} e^{ik_x x} dx \int_{|x|}^{\infty} p(\rho) \frac{\rho}{\sqrt{\rho^2 - x^2}} d\rho. \quad (\text{A-1})$$

Interchanging the order of integrations yields

$$\hat{p}(k_x) = 2 \int_0^{\infty} p(\rho)\rho d\rho \int_{-\rho}^{\rho} \frac{e^{ik_x x}}{\sqrt{\rho^2 - x^2}} dx. \quad (\text{A-2})$$

Define a new integration variable  $\phi$  according to

$$x = \rho \cos \phi, \quad (\text{A-3a})$$

or

$$\phi = \arccos \left( \frac{x}{\rho} \right) \quad (\text{A-3b})$$

and

$$d\phi = \frac{-dx}{\sqrt{\rho^2 - x^2}}. \quad (\text{A-3c})$$

Hence,

$$\hat{p}(k_x) = 2 \int_0^{\infty} p(\rho)\rho d\rho \int_0^{\pi} e^{ik_x \rho \cos \phi} d\phi, \quad (\text{A-4})$$

or, using Abramowitz and Stegun (1970, equation 9.1.21),

$$\hat{p}(k_x) = 2\pi \int_0^{\infty} p(\rho)J_0(k_x \rho)\rho d\rho, \quad (\text{A-5})$$

where  $J_0$  is the zeroth order Bessel function. Apart from the factor  $2\pi$ , equation (A-5) represents a zeroth order Hankel transform. Equation (10) can now be obtained by applying a temporal Fourier transform to both sides of equation (A-5).